

Review

Enhancing Single Molecule Imaging in Optofluidics and Microfluidics

Andreas E. Vasdekis * and Gregoire P.J. Laporte

Optics Laboratory, School of Engineering, Ecole Polytechnique Fédérale de Lausanne (EPFL), Lausanne CH-1015, Switzerland; E-Mail: gregoire.laporte@epfl.ch

* Author to whom correspondence should be addressed; E-Mail: andreas.vasdekis@epfl.ch; Tel.: +41-21-69-33742; Fax: +41-21-69-36930.

Received: 31 March 2011; in revised form: 23 May 2011 / Accepted: 25 July 2011 /

Published: 12 August 2011

Abstract: Microfluidics and optofluidics have revolutionized high-throughput analysis and chemical synthesis over the past decade. Single molecule imaging has witnessed similar growth, due to its capacity to reveal heterogeneities at high spatial and temporal resolutions. However, both resolution types are dependent on the signal to noise ratio (SNR) of the image. In this paper, we review how the SNR can be enhanced in optofluidics and microfluidics. Starting with optofluidics, we outline integrated photonic structures that increase the signal emitted by single chromophores and minimize the excitation volume. Turning then to microfluidics, we review the compatible functionalization strategies that reduce noise stemming from non-specific interactions and architectures that minimize bleaching and blinking.

Keywords: optofluidics; microfluidics; single molecule; fluorescence; imaging; surface passivation; micro-fabrication; lab-on-a-chip

1. Introduction

Since the first attempts at low temperature [1,2], near [3] or far field [4–7] single molecule imaging has evolved into a very powerful method of unmasking dynamic heterogeneities of complex material [8] or biological systems [9,10]. In the majority of cases, single molecule imaging takes place in fluorescence; in this imaging modality, light at a specific wavelength is absorbed by the

molecule, which in turn emits a Stokes-shifted signal. This signal is collected via high numerical-aperture optics and projected onto a sensitive imaging charge coupled device sensor (CCD), thus enabling its localization. It is worth noting that imaging is part of the much broader field of single molecule detection (SMD), where techniques such as Fluorescence Correlation Spectroscopy (FCS), spectroscopy and general optical sensing enable the detection of the presence and the activity of single molecules but not necessarily their localization [11].

Single molecule imaging has been particularly aided by the possibility of transgenically inducing light emission capabilities in living organisms [12–14], but also by more recent efforts of sequencing [15–17] and superresolution. Superresolution can be based on spectral multiplexing [18], digitization for localization [19,20], singlet state population manipulation (STED) [21], and time multiplexing via polarization [22], or photoactivation [23–26]. Apart from recent efforts in probing single fluorescent proteins in solution using electrokinetic traps [27] and more traditional ones like FCS [28], the vast majority of single molecule imaging studies take place on surfaces. Microfluidic systems are synergetic to this detection principle as they are compatible with many anchoring chemistries, but simultaneously enable variable delivery of bioentities, thus achieving unsurpassed levels of multiplexing [29,30].

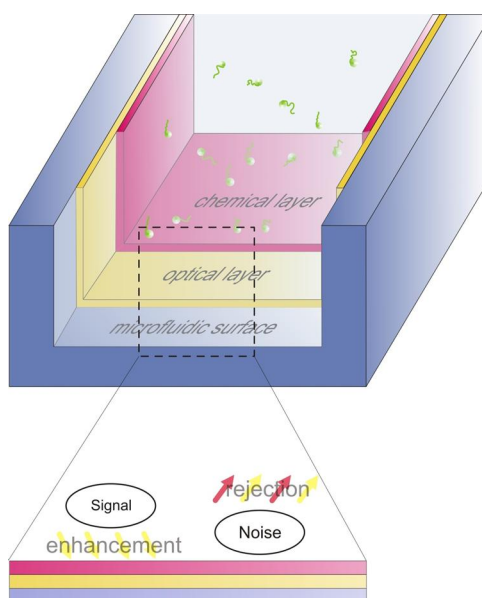
Microfluidics manipulates liquids at sub-millimeter length scales, enabling reduced reagent consumption and highly multiplexed studies by lithographically defining microfluidic channels in close proximity to each other. To this end, it has attracted substantial attention the past years in fundamental studies [31], as well as a wide range of applications, including microscale analysis systems [32–36], information processing [37,38], bioentity manipulation [39–41], and chemical synthesis [42]. Common materials for fabricating microfluidics are glass [35,43] and elastomeric polymers, such as the poly(dimethylsiloxane) (PDMS) [44]. While both materials are transparent in the visible range, PDMS exhibits relatively more advantages as it is more cost-effective, compatible with replica-molding, and its elastomeric nature enables flow control and object manipulation [45].

More recently, optofluidics emerged as the fusion of integrated optics with microfluidics [46,47], aiming primarily at novel photonic structures, such as light sources [48], waveguides [28] and optical modulators [49], as well as analytical methods, such as mass transport [50], on-chip imaging [51] and molecular manipulation [52]. More relevant to the present work is the recent report on surface optofluidics, where surfaces undertake an optical or chemical character to enable or enhance optofluidic functions [53].

Within this paper, we review recent reports on enhancing the signal to noise ratio during single molecule imaging in optofluidics and microfluidics (Figure 1). One way to achieve this type of enhancement is by increasing the signal emitted by single chromophores that reach the detector. We will review such methods in the optofluidic section (Section 2), highlighting the photonic structures that can be integrated with microfluidic channels. Similar performance enhancement can be achieved by minimizing the signal detected due to the presence of un-wanted molecules in the observation volume. To address this, there are in general two approaches. The first approach relates to the reduction of the observation volume, which can be achieved by both optofluidics (Section 2) and chemical techniques (Section 3). The second approach relates to the reduction of non-specific interactions, or equivalently the minimization of the number of un-wanted molecules within the

observation volume. This is reviewed in section 4, where the related chemical strategies compatible with microfluidics are discussed.

Figure 1. Upper: a general schematic illustrating the aim of this work: we review the optical and chemical layers compatible with conventional microfluidics that enhance the signal to noise ratio during single molecule imaging. **Lower:** This enhancement is achieved by decreasing the noise stemming from non-specific interaction (chemical layer), and by enhancing the signal via modifications of the electromagnetic and electrostatic environment of the single emitter (optical layer).



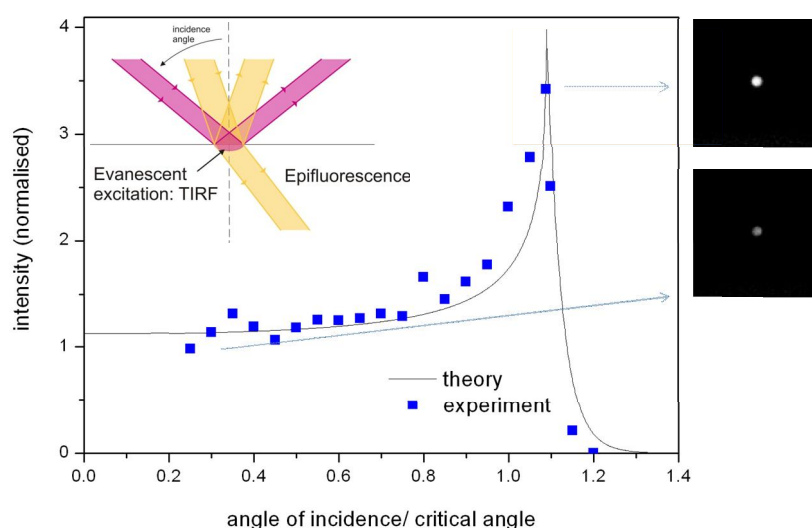
2. Signal to Noise Ratio Enhancement in Optofluidics

Multiple methods have been developed to push the fluorescence detection by employing photonic structures [54–56]. Such photonic structures exhibit a certain resonance frequency bandwidth; within this bandwidth they can passively either amplify light and/or modify its radiation pattern. Light in both cases can be either incident on such structures or be internally generated within them. In this paper, we will focus on the integration of such photonic structures with microfluidics. Such optofluidic examples involve the ‘zero mode waveguide’ [57], integrated ARROW waveguides for FCS [58], and evanescent wave resonators [52,59,60]. We will highlight however only optofluidic methods for single molecule imaging and localization; such optofluidic principles are mostly related to one or a combination of the following:

1. Confinement of the excitation volume to reduce the background;
2. Confinement of the excitation density to enhance the pumping rate;
3. Modification of the radiative and non-radiative rates of the chromophores;
4. Scattering enhancement and optical loss minimization to increase the signal reaching the detector;
5. Modification of the emission pattern in order to improve the collection efficiency.

Total internal reflection microscopy (TIRF) is one of the most conventional methods for fluorescence signal enhancement and, due to its compatibility with microfluidics, will be reviewed first for completeness, followed by methods to enhance the fluorescence emission by either employing metallic or dielectric micro- and nanostructures. In TIRF, evanescent waves are generated when light is totally reflected at the interface between two dielectric media (inset of Figure 2). The evanescent wave decays exponentially from the interface and thus selectively illuminates fluorophores in the close proximity to the interface (100's nm) [61,62]. The most common TIRF configurations use a prism [55,63], or a high NA objective [64,65]. The excitation intensity and the resulting fluorescent signal [61,66] are several times stronger in the TIRF condition than in epifluorescence (Figure 2). This enhancement can be estimated by using the Fresnel equations [64,67,68] and is synergetic to the coupling to surface modes, known as the Goos-Hänchen shift. In Figure 2, the intensity of the surface wave is plotted at different angles of incidence and is compared to an experimental measurement.

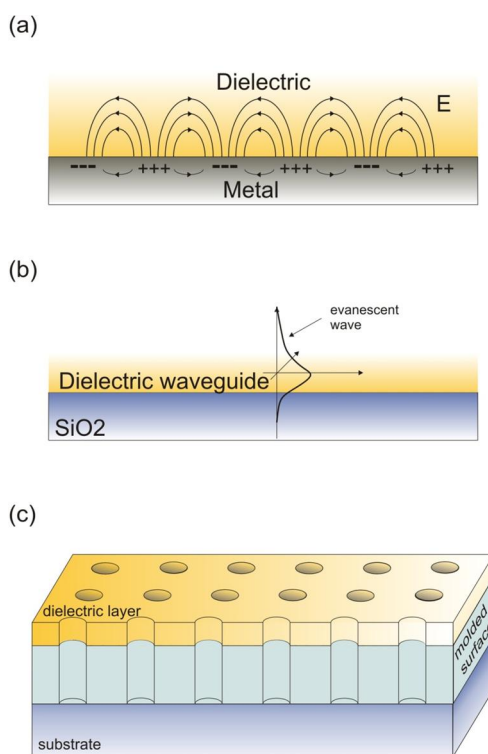
Figure 2. Characteristic intensity enhancement around the critical angle at the interface ($0.2 \cdot \lambda$) between a glass-coverslip and water (the wavelength is 488 nm). The experimental curve is the integrated signal of fluorescently labeled polystyrene beads (diameter of $0.8 \mu\text{m}$) adsorbed on the coverslip surface and coated with a water droplet; the theoretical one is the evanescent wave intensity at the water-glass interface, calculated from [67]. The inset illustrates the geometries of epifluorescence and total internal reflection.



An optofluidics-related approach to enhance the emission signal from single molecules is to employ surface plasmon polaritons (SPPs); these too are surface waves that only occur at the interface between a conductor and a dielectric [69] (Figure 3a). SPPs are excited when incident light interacts with the conductor's free charges that in turn collectively oscillate in resonance with the light wave. SPPs propagate along the conductor/external medium interface and the capability to structure such interfaces at the nanometer scale can lead to their strong resonant localization, primarily stemming from constructive interference. Plasmonic fluorescence enhancement has been demonstrated in a wide range of architectures, such as nanoparticles [70–74], nanowires [75], thin films [76], lithographically defined single [77–79] or composite nanostructures [80–82]. There are many excellent reviews on the

topic [83–86], so we shall only highlight the most recent advances and the advantages and disadvantages of this method.

Figure 3. An illustration of the optofluidic technologies, highlighted in the text, namely (a) surface plasmon polaritons, which are surface waves propagating at a dielectric metal interface (+ and – stand for regions where the charge density is lower and higher, respectively); In (b), a basic dielectric waveguide is shown, comprising of a thin dielectric layer where the waves propagate; In (c), a schematic representation of a photonic crystal device is shown. The surface on the substrate is lithographically molded with the periodic structure and the thin dielectric layer is sputtered on the top.



The most common mechanisms involved in plasmonic fluorescence enhancement are higher scattering efficiency due to the metal presence, denser excitation localization and thus pumping rate, and increased radiative rate due to the change in the photonic environment of the isolated chromophore [72,87]. Most recently, an enhancement of 1340 was reported using bow-tie antennas [78]; these are lithographically defined plasmonic nanostructures with typical maximum dimensions in the range of 100's nm with the capacity of strongly localizing the excitation field at their centre. Similar principles have recently found applications in non-linear imaging, by coating nanoparticles with a metal layer [88]. Typical disadvantages regarding plasmonic fluorescence enhancement are its inverse relationship to the emitter's quantum efficiency, and the substantial quenching that occurs when the chromophore is closer to the metal surface [89,90]. Another disadvantage of plasmonic resonators is their small size, which in turn substantially reduces the field of view. In addition, the integration of metallic structures with PDMS microfluidics may suffer from inefficient sealing, requiring the use of a specifically patterned metal layer or coating with a patterned polymer layer [91] in order to eliminate the contact between PDMS and metallic surfaces.

Dielectric resonators coupled with single emitters have been also explored primarily within the context of quantum electrodynamics (QED) [92,93]. Similar principles have been applied to fluorescent imaging, albeit in the weak-coupling regime. One such dielectric architecture is thin films integrated immediately below the surface of interest (Figure 3b). One such embodiment is employed in TIRF, where films with appropriate optical properties and dimensions are used to resonantly enhance the evanescent field of totally internally reflected incident light via coupling to waveguide modes supported by the film [94–98]. Thin films can also be directly employed as waveguides, forming an integrated version of TIRF [99,100]; in these schemes light is end-coupled to the waveguide so that its evanescent intensity excites the fluorophores in the waveguide's vicinity. More recently, a thin film was employed as an antenna, enhancing the collection efficiency to approximately 100% [101]. In this case, the emitters are embedded in a thin polymer layer, sandwiched between a higher index medium layer (sapphire) and air. The high index medium forces the emitted light to refract at smaller angles, thereby enhancing the collection efficiency.

Periodic dielectric structures have also found applications in fluorescent enhancement. One such example is stacks of thin films, which exhibit very high Bragg reflectivity within a certain wavelength range. When single molecules are placed in the proximity of such structures and their emission spectrum overlaps with the mirror resonance, the spectrum and spontaneous emission rate can be substantially modified and enhanced, respectively [102,103]. Photonic crystals are another type of periodic dielectric structures that have been explored to the same end (Figure 3c). These are in most cases lithographically defined in high index dielectrics with minimal absorption in the wavelength range of interest. If carefully selected, their periodicity can impose a phase matching condition for both the excitation and emission wavelength [104–107]. The operational principle is based on the coupling of both the external pump and the fluorescence signal into Bloch wave modes; these modes are 'leaky' modes, manifested by their strong evanescent near fields on the surface of the photonic crystal, which is critical to enhancing the excitation and emission extraction. Very recently, annular Bragg resonators for focusing the excitation light have been demonstrated, exhibiting an enhancement factor of 20 [108]. Colloidal microspheres, have been also employed, initially within the context of QED [109]. Recently, sub-wavelength focusing was demonstrated by illuminating latex microspheres with Gaussian beams; this high excitation confinement resulted in a 5-fold enhancement of the single molecule fluorescence [110]. Another practical effect of colloidal microspheres is the improvement in extraction by redirecting the light emitted at large angles toward the normal to the surface [103]. More recently, the possibility to replace high-NA oil immersion objectives with colloidal particles was demonstrated [111]; the use of low-NA objective lenses enabled high temperature and high photostability single molecule imaging. We note that dielectrics can be integrated with PDMS microfluidics due to the presence of a native oxide layer on their surfaces or their direct compatibility with O₂ plasma (e.g., polymers).

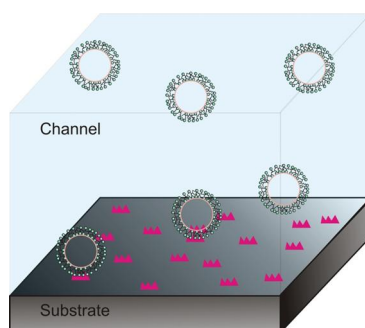
3. Microfluidic Architectures for Minimizing Photobleaching and the Excitation Volume

One advantage of single molecule imaging is the higher time-domain resolution in interrogating molecular dynamics than is possible in ensemble studies. However, this can be hampered by the photostability of singlet exciton emission, due to O₂ and intersystem crossing mediated bleaching and blinking. The latter gives rise to stochastic fluctuations not linked to the biological behavior itself.

These challenges have been addressed in microfluidics by mixing oxygen scavengers and triplet quenchers in the imaging buffer [112], which recently, under careful design, enabled the shortest observation duration [113]. An alternative approach integrating the imaging channels with ones continuously ventilated with nitrogen was recently demonstrated [114]. Deoxygenation was possible due to the porous nature of PDMS, thus enabling measurements in the absence of the aforementioned enzymes that can interfere with biological activity [114]. Another possible time-domain resolution limitation, especially in single molecule fluorescence energy transfer (smFRET), is the fluidic speed that can be relatively high especially during fluidic mixing. Sophisticated microfluidic architectures can address this by reducing the flow velocities immediately after mixing, thereby enabling longer optical interrogations [115].

Confocal imaging exhibits superior sensitivity by significantly restricting the excitation volume and thus minimizing the background fluorescence [4,116,117]. Microfluidic and nanofluidic systems can in principle achieve the same and push the limits of fluorescence detection. Within this paper, we will focus on the former, as many excellent reviews exist on the latter [118–120]. Apart from reduced size microfluidic channels employed in a recent report of multidimensional investigation of molecular energy landscapes and activities [30], volume restriction can be achieved by using micro-droplets [42,121]. The latter have not yet found widespread applications in single molecule imaging, contrary to vesicle encapsulation, which additionally exhibits much smaller volumes and the possibility of surface tethering [122–123]. In addition to the very small observation volumes, vesicle encapsulation (figure 4) enables the exclusion of any interaction of the contained molecules with the environment (including the surface), and as the possibility to combine surface immobilization with molecular recognition mechanisms, such as sequence specificity, thus forming a single molecule sensor of unlabeled oligonucleotides [124].

Figure 4. An illustration of vesicles tethered on a microfluidic surface and vesicles that freely float inside the bulk volume of the micro-channel.



4. Noise Reduction Using Microfluidic Compatible Surface Passivation Strategies

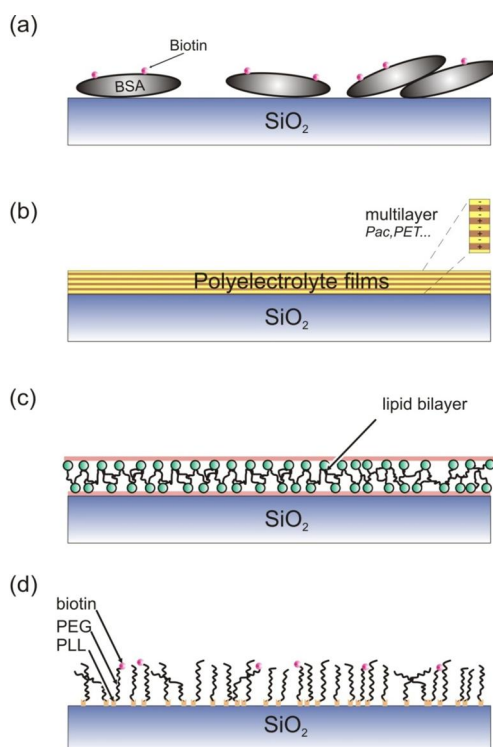
Adhesion to biomaterials has been explored for many years, primarily focusing on the development of surfaces capable of non-specific protein adsorption for applications in implants, contact lenses and bioassays. Similar challenges have also been addressed in microfluidics. Microfluidic surfaces can act as anchoring points, where the molecules under investigation are immobilized. As discussed in the introduction, these attachment points need to exhibit certain properties in order to enhance the imaging of single molecules. In addition to their capacity to attract the ‘signal molecules’ with high affinity and

resist non-specific adsorption of molecules that can contribute to noise [125–128], there are additional properties that we summarize below:

1. Simplicity and minimal preparation requirements: Single molecule imaging and detection is becoming a substantially interdisciplinary field, comprised of biologists, physicists and chemists. Hence, synergetic also to microfluidics, the chemical modification needs to be simple and require few implementation steps;
2. Compatibility with microfluidic fabrication: this necessitates that the surface chemistry is not compromised during fabrication, but also that the microfluidics retain their properties (e.g., mechanical) during surface treatment;
3. Bioactivity: The immobilized biomolecules must retain their activity, for example a protein that can unfold and refold, or a nucleic acid that can be recognized by site-specific proteins.

Depending on the type of microfluidic devices and their fabrication, surfaces can be modified via a variety of chemistries. It is widely accepted that no single chemistry is compatible with multiple single molecule imaging analyses. Herein, we will not discuss gel confinement via polymerization [129,130] due to its contradiction to one of the main microfluidic advantages, namely that of flow-based delivery and multiplexing. On the contrary, we will focus on processes that can be performed either in-situ or ex-situ and comply with the aforementioned ‘ideal’ properties (Figure 5).

Figure 5. An illustration of some common surface passivation schemes in microfluidics: bovine albumin (BSA) adsorption (a), polyelectrolyte films (b), lipid bilayers (c) and PLL-g- poly(ethylene glycol) (PEG) copolymers.

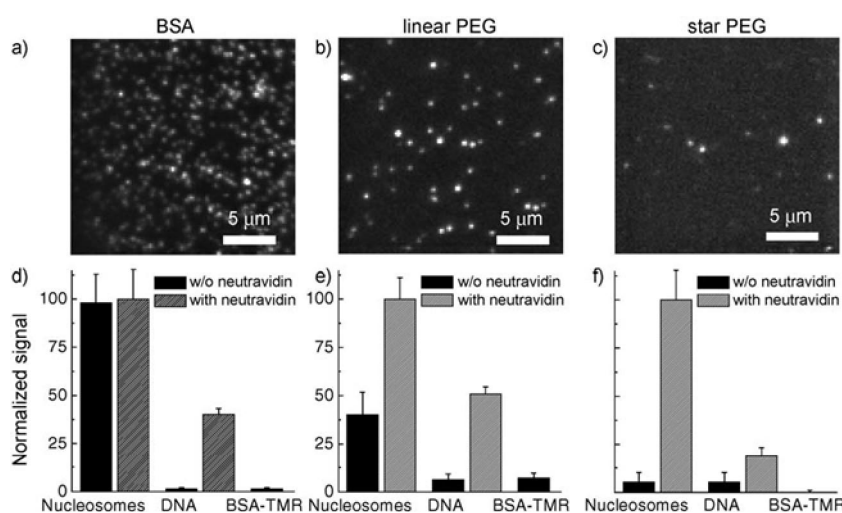


Self-assembly (SAM) and self-organization of molecular films have also been extensively reported. One area is the creation of monolayers of alkyl chains on thin gold films [131]. While such techniques

are especially important in surface plasmon resonance measurements (SPR), more recently similar approaches have been proposed for PDMS, the cornerstone medium for microfluidics. In the latter, the PDMS pre-polymer is mixed with small molecules and then cast against a template with a specific surface energy [132,133]. During cross-linking, the small molecules in the PDMS solution are driven to the surface in order to match the energy of the mold surface. This method is particularly pertinent for the creation of chemical patterns, however to the authors' knowledge the bonding with micro-channels is rather challenging to achieve using such surface treated templates.

A more common method to avoid non-specific interactions, is to pre-coat the surface with strongly adhering proteins. Subsequently, the resulting formed thin protein layer blocks in turn the surface recognition by other molecules. A typical protein of this type is bovine albumin (BSA) [134], which can be biotinylated, providing thus the possibility of a biotin-streptavidin linkage (Figure 5a). This technique is rather straightforward to implement and can be performed in situ, once the microfluidics or flow channels have been realized. However, it has been shown that the technique does not exhibit the highest level of non-specific adsorption prevention [126] and to also potentially interfere with the kinetics of immobilized molecules, such as ribozymes [127,135] (Figure 6).

Figure 6. Upper: Images illustrating the non-specific binding on labeled nucleosomes on coverslips coated with BSA (a), PEG (b) and star-PEG (c). **Lower:** Quantification based on the number of fluorescent spots. Image used with permission from [126].



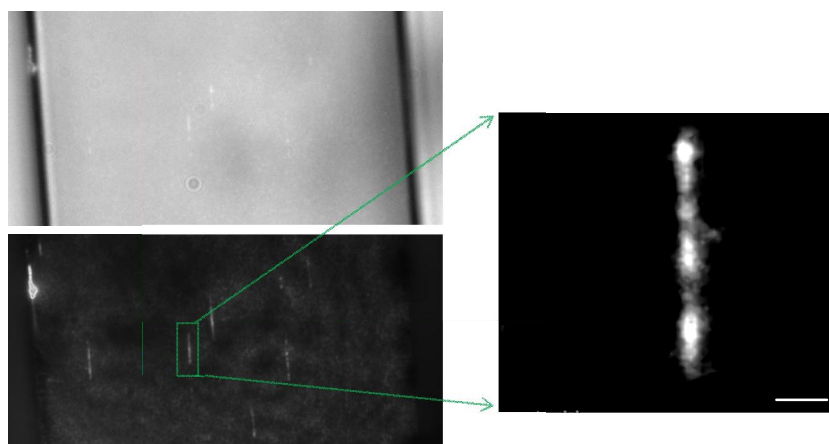
An alternative approach for in-situ passivation of microchannels was recently demonstrated by Illumina in single molecule sequencing [136]. The technique involved the polymerization of acrylamide in glass capillaries and exhibited significant prevention against non-specific recognition, high sensitivity in isolated nucleic acid imaging, as well as stability over repeated polymerase chain reactions (PCR) [128]. With regards to single molecule DNA sequencing, another technique is based on the use of polyelectrolyte films (Figure 5b). One report focused on the use of single polyacrylic acid layers and was shown to exhibit low tendency to attract fluorescently labeled bases [137]. Multiple films can also be used [15,138,140]. Polyelectrolyte multi-layer films effectively tune the charge density of the substrate and thus exhibit the capacity to repel molecules with the same charge via electrostatic interactions.

Similar strategies of in-situ passivation of PDMS microchannels involve the use of the Pluronic copolymer [141,142]. However, most Pluronic treatment applications focus on the use of microfluidics as cell-culture systems. As an alternative, individual components of the Pluronic block-copolymers, namely poly(ethylene oxide) grafted on oxide surfaces, have been extensively studied in single molecule imaging. Such passivation treatments were shown to exhibit near zero adsorption both when the polymer exhibits linear and star-shape form and exhibit bioactivity evidenced by the reversible denaturation and renaturation of immobilized ribonucleases H (RNase H) [143,144]. However, grafting of PEO requires the surface treatment with aminosilanes, which can exhibit certain disadvantages for in-situ passivation, especially when used with PDMS which swells under treatment with organic solvents [145].

Supported lipid bilayers have also been extensively explored as protein resistant surfaces for single molecule studies (Figure 5c) [146]. In addition to their bio-fouling properties, bilayers exhibit a chemical nature that simulates that of the cellular environment and as a result specifically immobilized biomolecules are expected to maintain their bioactivity [146]. Such membranes are commonly spontaneously assembled from small unilamellar vesicles [147]. Once formed, these bilayers behave like true two-dimensional fluids and any molecules residing on them diffuse freely in the surface plane [148]. Such architectures have found substantial applications within the area of DNA manipulation and stretching by flow [149,150]. In these experiments, highly ordered DNA arrays are formed at localized microscale lipid diffusion barriers, forming thus an elegant assay for highly multiplexed nucleic acid structural studies [151]. On the contrary, dehydration, e.g. occurring during molecular combing, may be considered a disadvantage of this method.

The final surface functionalization approach we will discuss and possibly the most common one is poly(ethylene glycol) (PEG) (Figure 5d). PEG has been characterized as the benchmark in resistance of non-specific interactions via steric hindrance and has found a plethora of applications in implants, cell cultures, microfluidics and protein circulation in vivo [152–156]. PEG however does not react with untreated surfaces, thus necessitating an additional surface treatment step. One method is to perform the functionalization ex-situ and then fabricate the microfluidic channels [157]; however, many microfluidic architectures, especially lithographically defined ones, are not compatible with this method as they require the invasive step of bonding and sealing. As a result, several methods have been developed to address this and perform in-situ PEGylation of microfluidic surfaces. Physisorption with PEG copolymers is one of the simplest ones, and involves only the incubation of aqueous buffers of the copolymer. Poly(L-lysine)-g-poly(ethylene glycol) (PLL-g-PEG) is one such copolymer, which has found numerous applications in both oxide and PDMS based microfluidics for cell cultures, protein studies and single molecule manipulation and imaging [40,153,158,159] (Figure 7). An alternative PEG surface functionalization is based on the covalent bonding of PEG to albumin microgels, which are recognized by the surface [160]. This technique however remains to be fully explored in single molecule imaging applications. Despite recent efforts, little has been achieved specifically in replacing PEG. One such example is dextran [161], which however requires additional efforts to render the functionalization process less toxic [162].

Figure 7. Left: Microscopy images of combed λ -phage DNA molecules on a PLL-g-PEG coated microfluidic surfaces; the upper and bottom images are under white light and fluorescent conditions respectively. **Right:** An optically magnified image of an individual nucleic acid; the scale bar is 1 μm . In these experiments, the copolymer aided both the prevention of non-specific interactions, but also the stretching of the DNA below its contour length due to the hydrophilic nature of the PEG [40].



Alternative means for *in situ* PEGylation of microfluidic surfaces involves direct grafting, usually by first treating the microfluidic surface and subsequently introducing the PEG solution. These processes are usually laborious and require long surface treatments that can interfere with the stability of the microchannels; however they have been shown to provide uniform and extremely stable functionalized surfaces [163–165]. Star-PEG has been used with similar methods, and shown to exhibit superior protein adsorption resistance due to its higher surface coverage and thickness (Figure 6) [126,166]. Alternative techniques of functionalizing surfaces with PEG involve directly mixing the PDMS prepolymer with PEG additives terminated with appropriate end groups [167,168], or by photografting [169,170], which also poses an elegant method for *in-situ* creating chemical patterns. Finally, the direct imprinting of PEG films with microchannels has been reported with some excellent results on non-biofouling, albeit with reported challenges in bonding and sealing [171,172].

5. Conclusions

We have reviewed a wide range of methods for enhancing the signal to noise ratio of single molecule imaging in microfluidics. Photonic structures can be directly integrated in the vicinity of micro-channels, forming thus optofluidic platforms that both minimize the background and enhance the signal. Multiple such structures exist that can be adopted for different fluorophores and types of measurements. When choosing, care needs to be taken in order not to substantially modify the photophysical properties of the labels, or if desired, to do it in a controlled way. Due to their fabrication simplicity (bottom-up mostly), plasmonic resonators have been explored more than dielectric ones for single molecule detection; however, recent reports demonstrate the possibility of achieving comparable performances.

With regards to microfluidic approaches, we reviewed architectures that can enhance the sensitivity in single molecule imaging. The latter was mostly related to time domain resolution, stability, and

volume restriction methods for adapting the confocal principle in microfluidics. Finally, common surface passivation methods were reviewed; in general, there is no ideal procedure applicable to all types of single molecule experiments. We have attempted to highlight the most popular techniques that are synergetic to microfluidics, both in terms of fabrication and simplicity. One exciting emerging concept to this end is the aptamer surface functionalization [173]; however, apart from affinity extractions and separations, little has been reported within the context of single molecule imaging.

Acknowledgements

We are grateful to Demetri Psaltis for fruitful and inspiring discussions; in addition, we acknowledge the assistance we received by Aleksandra Radenovic and members of her group for the DNA related experiments and many discussions on TIRF microscopy.

References

1. Moerner, W.E.; Kador, L. Optical detection and spectroscopy of single molecules in a solid. *Phys. Rev. Lett.* **1989**, *62*, 2535–2538.
2. Orrit, M.; Bernard, J. Single pentacene molecules detected by fluorescence excitation in a para-terphenyl crystal. *Phys. Rev. Lett.* **1990**, *65*, 2716–2719.
3. Betzig, E.; Chichester, R.J. Single molecules observed by near-field scanning optical microscopy. *Science* **1993**, *262*, 1422–1425.
4. Nie, S.M.; Chiu, D.T.; Zare, R.N. Probing individual molecules with confocal fluorescence microscopy. *Science* **1994**, *266*, 1018–1021.
5. Macklin, J.J.; Trautman, J.K.; Harris, T.D.; Brus, L.E. Imaging and time-resolved spectroscopy of single molecules at an interface. *Science* **1996**, *272*, 255–258.
6. Xie, X.S. Single-molecule spectroscopy and dynamics at room temperature. *Acc. Chem. Res.* **1996**, *29*, 598–606.
7. Weiss, S. Measuring conformational dynamics of biomolecules by single molecule fluorescence spectroscopy. *Nat. Struct. Biol.* **2000**, *7*, 724–729.
8. Lupton, J.M. Single-molecule spectroscopy for plastic electronics: Materials analysis from the bottom-up. *Adv. Mater.* **2010**, *22*, 1689–1721.
9. Moerner, W.E. New directions in single-molecule imaging and analysis. *Proc. Natl. Acad. Sci. USA* **2007**, *104*, 12596–12602.
10. Joo, C.; Balci, H.; Ishitsuka, Y.; Buranachai, C.; Ha, T. Advances in single-molecule fluorescence methods for molecular biology. *Annu. Rev. Biochem.* **2008**, *77*, 51–76.
11. Lakowicz, J.R. *Principles of Fluorescence Spectroscopy*; Springer: New York, NY, USA, 2006.
12. Shimomura, O.; Johnson, F.H.; Saiga, Y. Extraction, purification and properties of Aequorin, a bioluminescent protein from luminous hydromedusan Aequorea. *J. Cell. Comp. Physiol.* **1962**, *59*, 223–239.
13. Chalfie, M.; Tu, Y.; Euskirchen, G.; Ward, W.W.; Prasher, D.C. Green fluorescent protein as a marker for gene expression. *Science* **1994**, *263*, 802–805.
14. Giepmans, B.N.G.; Adams, S.R.; Ellisman, M.H.; Tsien, R.Y. The fluorescent toolbox for assessing protein location and function. *Science* **2006**, *312*, 217–224.

15. Braslavsky, I.; Hebert, B.; Kartalov, E.; Quake, S.R. Sequence information can be obtained from single DNA molecules. *Proc. Natl. Acad. Sci. USA* **2003**, *100*, 3960–3964.
16. Fuller, C.W.; Middendorf, L.R.; Benner, S.A.; Church, G.M.; Harris, T.; Huang, X.H.; Jovanovich, S.B.; Nelson, J.R.; Schloss, J.A.; Schwartz, D.C.; *et al.* The challenges of sequencing by synthesis. *Nat. Biotechnol.* **2009**, *27*, 1013–1023.
17. Flusberg, B.A.; Webster, D.R.; Lee, J.H.; Travers, K.J.; Olivares, E.C.; Clark, T.A.; Korlach, J.; Turner, S.W. Direct detection of DNA methylation during single-molecule, real-time sequencing. *Nat. Methods* **2010**, *7*, 461–465.
18. van Oijen, A.M.; Kohler, J.; Schmidt, J.; Muller, M.; Brakenhoff, G.J. 3-Dimensional super-resolution by spectrally selective imaging. *Chem. Phys. Lett.* **1998**, *292*, 183–187.
19. Thompson, R.E.; Larson, D.R.; Webb, W.W. Precise nanometer localization analysis for individual fluorescent probes. *Biophys. J.* **2002**, *82*, 2775–2783.
20. Yildiz, A.; Forkey, J.N.; McKinney, S.A.; Ha, T.; Goldman, Y.E.; Selvin, P.R. Myosin V walks hand-over-hand: Single fluorophore imaging with 1.5-nm localization. *Science* **2003**, *300*, 2061–2065.
21. Hell, S.W.; Wichmann, J. Breaking the diffraction resolution limit by stimulated emission-stimulated emission depletion fluorescence microscopy. *Opt. Lett.* **1994**, *19*, 780–782.
22. Testa, I.; Schonle, A.; Middendorff, C.V.; Geisler, C.; Medda, R.; Wurm, C.A.; Stiel, A.C.; Jakobs, S.; Bossi, M.; Eggeling, C.; *et al.* Nanoscale separation of molecular species based on their rotational mobility. *Opt. Express* **2008**, *16*, 21093–21104.
23. Betzig, E. Proposed method for molecular optical imaging. *Opt. Lett.* **1995**, *20*, 237–239.
24. Hess, S.T.; Girirajan, T.P.K.; Mason, M.D. Ultra-high resolution imaging by fluorescence photoactivation localization microscopy. *Biophys. J.* **2006**, *91*, 4258–4272.
25. Rust, M.J.; Bates, M.; Zhuang, X.W. Sub-diffraction-limit imaging by stochastic optical reconstruction microscopy (STORM). *Nat. Methods* **2006**, *3*, 793–795.
26. Sharonov, A.; Hochstrasser, R.M. Wide-field subdiffraction imaging by accumulated binding of diffusing probes. *Proc. Natl. Acad. Sci. USA* **2006**, *103*, 18911–18916.
27. Goldsmith, R.H.; Moerner, W.E. Watching conformational- and photodynamics of single fluorescent proteins in solution. *Nat. Chem.* **2010**, *2*, 179–186.
28. Rudenko, M.I.; Kuhn, S.; Lunt, E.J.; Deamer, D.W.; Hawkins, A.R.; Schmidt, H. Ultrasensitive Q beta phage analysis using fluorescence correlation spectroscopy on an optofluidic chip. *Biosens. Bioelectron.* **2009**, *24*, 3258–3263.
29. Taniguchi, Y.; Choi, P.J.; Li, G.W.; Chen, H.Y.; Babu, M.; Hearn, J.; Emili, A.; Xie, X.S. Quantifying *E-coli* Proteome and Transcriptome with Single-Molecule Sensitivity in Single Cells. *Science* **2010**, *329*, 533–538.
30. Kim, S.; Streets, A.M.; Lin, R.R.; Quake, S.R.; Weiss, S.; Majumdar, D.S. High-throughput single-molecule optofluidic analysis. *Nat. Methods* **2011**, *8*, 242–245.
31. Squires, T.M.; Quake, S.R. Microfluidics: Fluid physics at the nanoliter scale. *Rev. Mod. Phys.* **2005**, *77*, 977–1026.
32. Reyes, D.R.; Iossifidis, D.; Auroux, P.A.; Manz, A. Micro total analysis systems. 1. Introduction, theory, and technology. *Anal. Chem.* **2002**, *74*, 2623–2636.

33. Stone, H.A.; Stroock, A.D.; Ajdari, A. Engineering flows in small devices: Microfluidics toward a lab-on-a-chip. *Annu. Rev. Fluid Mech.* **2004**, *36*, 381–411.
34. Burns, M.A.; Johnson, B.N.; Brahmamandra, S.N.; Handique, K.; Webster, J.R.; Krishnan, M.; Sammarco, T.S.; Man, P.M.; Jones, D.; Heldsinger, D.; *et al.* An integrated nanoliter DNA analysis device. *Science* **1998**, *282*, 484–487.
35. Effenhauser, C.S.; Manz, A.; Widmer, H.M. Glass chips for hisgh speed capillary electrophoresis separations with submicrometer plate heights. *Anal. Chem.* **1993**, *65*, 2637–2642.
36. Maerkl, S.J. Next generation microfluidic platforms for high-throughput protein biochemistry. *Curr. Opin. Biotechnol.* **2011**, *22*, 59–65.
37. Prakash, M.; Gershenfeld, N. Microfluidic bubble logic. *Science* **2007**, *315*, 832–835.
38. Weaver, J.A.; Melin, J.; Stark, D.; Quake, S.R.; Horowitz, M.A. Static control logic for microfluidic devices using pressure-gain valves. *Nat. Phys.* **2010**, *6*, 218–223.
39. Di Carlo, D.; Wu, L.Y.; Lee, L.P. Dynamic single cell culture array. *Lab Chip* **2006**, *6*, 1445–1449.
40. Vasdekis, A.E.; O'Neil, C.P.; Hubbell, J.A.; Psaltis, D. Microfluidic assays for DNA manipulation based on a block copolymer immobilization strategy. *Biomacromolecules* **2010**, *11*, 827–831.
41. Chung, K.; Kim, Y.; Kanodia, J.S.; Gong, E.; Shvartsman, S.Y.; Lu, H. A microfluidic array for large-scale ordering and orientation of embryos. *Nat. Methods* **2011**, *8*, 171–176.
42. Huebner, A.; Sharma, S.; Srisa-Art, M.; Hollfelder, F.; Edel, J.B.; Demello, A.J. Microdroplets: A sea of applications? *Lab Chip* **2008**, *8*, 1244–1254.
43. Stjernstrom, M.; Roeraade, J. Method for fabrication of microfluidic systems in glass. *J. Micromech. Microeng.* **1998**, *8*, 33–38.
44. Qin, D.; Xia, Y.N.; Whitesides, G.M. Soft lithography for micro- and nanoscale patterning. *Nat. Protoc.* **2010**, *5*, 491–502.
45. Unger, M.A.; Chou, H.P.; Thorsen, T.; Scherer, A.; Quake, S.R. Monolithic microfabricated valves and pumps by multilayer soft lithography. *Science* **2000**, *288*, 113–116.
46. Psaltis, D.; Quake, S.R.; Yang, C.H. Developing optofluidic technology through the fusion of microfluidics and optics. *Nature* **2006**, *442*, 381–386.
47. Monat, C.; Domachuk, P.; Eggleton, B.J. Integrated optofluidics: A new river of light. *Nat. Photonics* **2007**, *1*, 106–114.
48. Song, W.Z.; Vasdekis, A.E.; Li, Z.Y.; Psaltis, D. Optofluidic evanescent dye laser based on a distributed feedback circular grating. *Appl. Phys. Lett.* **2009**, *94*, doi:10.1063/1.3124652.
49. Cuennet, J.G.; Vasdekis, A.E.; De Sio, L.; Psaltis, D. Optofluidic modulator based on peristaltic nematogen microflows. *Nat. Photonics* **2011**, *5*, 234–238.
50. Liu, G.L.; Kim, J.; Lu, Y.; Lee, L.P. Optofluidic control using photothermal nanoparticles. *Nat. Mater.* **2006**, *5*, 27–32.
51. Cui, X.Q.; Lee, L.M.; Heng, X.; Zhong, W.W.; Sternberg, P.W.; Psaltis, D.; Yang, C.H. Lensless high-resolution on-chip optofluidic microscopes for *Caenorhabditis elegans* and cell imaging. *Proc. Natl. Acad. Sci. USA* **2008**, *105*, 10670–10675.

52. Yang, A.H.J.; Moore, S.D.; Schmidt, B.S.; Klug, M.; Lipson, M.; Erickson, D. Optical manipulation of nanoparticles and biomolecules in sub-wavelength slot waveguides. *Nature* **2009**, *457*, 71–75.
53. Vasdekis, A.E.; Cuennet, J.G.; Song, W.Z.; Choi, J.-W.; De Sio, L.; O'Neil, C.P.; Hubbell, J.A.; Psaltis, D. Surface optofluidics. In *Proceedings of SPIE Optics and Photonics*, San Diego, CA, USA, 1–5 August 2010; p. 776224.
54. Wenger, J.; Rigneault, H. Photonic methods to enhance fluorescence correlation spectroscopy and single molecule fluorescence detection. *Int. J. Mol. Sci.* **2010**, *11*, 206–221.
55. Walter, N.G.; Huang, C.Y.; Manzo, A.J.; Sobhy, M.A. Do-it-yourself guide: how to use the modern single-molecule toolkit. *Nat. Methods* **2008**, *5*, 475–489.
56. Hill, E.K.; de Mello, A.J. Single-molecule detection using confocal fluorescence detection: Assessment of optical probe volumes. *Analyst* **2000**, *125*, 1033–1036.
57. Levene, M.J.; Korlach, J.; Turner, S.W.; Foquet, M.; Craighead, H.G.; Webb, W.W. Zero-mode waveguides for single-molecule analysis at high concentrations. *Science* **2003**, *299*, 682–686.
58. Schmidt, H.; Hawkins, A.R. Optofluidic waveguides: I. Concepts and implementations. *Microfluid. Nanofluid.* **2008**, *4*, 3–16.
59. Armani, A.M.; Kulkarni, R.P.; Fraser, S.E.; Flagan, R.C.; Vahala, K.J. Label-free, single-molecule detection with optical microcavities. *Science* **2007**, *317*, 783–787.
60. Zhu, H.Y.; White, I.M.; Suter, J.D.; Zourob, M.; Fan, X.D. Opto-fluidic micro-ring resonator for sensitive label-free viral detection. *Analyst* **2008**, *133*, 356–360.
61. Paige, M.F.; Bjerneld, E.J.; Moerner, W.E. A comparison of through-the-objective total internal reflection microscopy and epifluorescence microscopy for single-molecule fluorescence imaging. *Single Mol.* **2001**, *2*, 191–201.
62. De Fornel, F. *Evanescent Waves: from Newtonian Optics to Atomic Optics*; Rhodes, W.T., Ed; Springer-Verlag: Berlin, Germany, 1997.
63. Axelrod, D. Total internal reflection fluorescence microscopy in cell biology. *Traffic* **2001**, *2*, 764–774.
64. Axelrod, D.; Burghardt, T.P.; Thompson, N.L. Total internal reflection fluorescence. *Annu. Rev. Biophys. Bioeng.* **1984**, *13*, 247–268.
65. Axelrod, D. Selective imaging of surface fluorescence with very high aperture microscope objectives. *J. Biomed. Opt.* **2001**, *6*, 6–13.
66. Carniglia, C.K.; Mandel, L.; Drexhage, K.H. Absorption and emission of evanescent photons. *J. Opt. Soc. Am.* **1972**, *62*, 479–486.
67. Lotsch, H.K.V. Beam displacement at total reflection - Goos Hanchen effect 1. *Optik* **1970**, *32*, 116–137.
68. Lai, H.M.; Cheng, F.C.; Tang, W.K. Goos-Hanchen effect around and off the critical angle. *J. Opt. Soc. Am. A* **1986**, *3*, 550–557.
69. Barnes, W.L.; Dereux, A.; Ebbesen, T.W. Surface plasmon subwavelength optics. *Nature* **2003**, *424*, 824–830.
70. Anger, P.; Bharadwaj, P.; Novotny, L. Enhancement and quenching of single-molecule fluorescence. *Phys. Rev. Lett.* **2006**, *96*, doi:10.1103/PhysRevLett.96.113002.

71. Kuhn, S.; Hakanson, U.; Rogobete, L.; Sandoghdar, V. Enhancement of single-molecule fluorescence using a gold nanoparticle as an optical nanoantenna. *Phys. Rev. Lett.* **2006**, *97*, doi:10.1103/PhysRevLett.97.017402.
72. Tam, F.; Goodrich, G.P.; Johnson, B.R.; Halas, N.J. Plasmonic enhancement of molecular fluorescence. *Nano Lett.* **2007**, *7*, 496–501.
73. Zhang, J.; Fu, Y.; Chowdhury, M.H.; Lakowicz, J.R. Metal-enhanced single-molecule fluorescence on silver particle monomer and dimer: Coupling effect between metal particles. *Nano Lett.* **2007**, *7*, 2101–2107.
74. Cang, H.; Labno, A.; Lu, C.G.; Yin, X.B.; Liu, M.; Gladden, C.; Liu, Y.M.; Zhang, X.A. Probing the electromagnetic field of a 15-nanometre hotspot by single molecule imaging. *Nature* **2011**, *469*, 385–388.
75. Taminiau, T.H.; Stefani, F.D.; Segerink, F.B.; Van Hulst, N.F. Optical antennas direct single-molecule emission. *Nat. Photonics* **2008**, *2*, 234–237.
76. Burghardt, T.P.; Charlesworth, J.E.; Halstead, M.F.; Tarara, J.E.; Ajtai, K. *In situ* fluorescent protein imaging with metal film-enhanced total internal reflection microscopy. *Biophys. J.* **2006**, *90*, 4662–4671.
77. Rigneault, H.; Capoulade, J.; Dintinger, J.; Wenger, J.; Bonod, N.; Popov, E.; Ebbesen, T.W.; Lenne, P.F. Enhancement of single-molecule fluorescence detection in subwavelength apertures. *Phys. Rev. Lett.* **2005**, *95*, doi:10.1103/PhysRevLett.95.117401.
78. Kinkhabwala, A.; Yu, Z.F.; Fan, S.H.; Avlasevich, Y.; Mullen, K.; Moerner, W.E. Large single-molecule fluorescence enhancements produced by a bowtie nanoantenna. *Nat. Photonics* **2009**, *3*, 654–657.
79. Aouani, H.; Itzhakov, S.; Gachet, D.; Devaux, E.; Ebbesen, T.W.; Rigneault, H.; Oron, D.; Wenger, J. Colloidal quantum dots as probes of excitation field enhancement in photonic antennas. *ACS Nano* **2010**, *4*, 4571–4578.
80. Song, J.H.; Atay, T.; Shi, S.F.; Urabe, H.; Nurmikko, A.V. Large enhancement of fluorescence efficiency from CdSe/ZnS quantum dots induced by resonant coupling to spatially controlled surface plasmons. *Nano Lett.* **2005**, *5*, 1557–1561.
81. Kim, K.; Kim, D.J.; Cho, E.J.; Suh, J.S.; Huh, Y.M.; Kim, D. Nanograting-based plasmon enhancement for total internal reflection fluorescence microscopy of live cells. *Nanotechnology* **2009**, *20*, doi:10.1088/0957-4484/20/1/015202..
82. Kravets, V.G.; Zorinians, G.; Burrows, C.P.; Schedin, F.; Geim, A.K.; Barnes, W.L.; Grigorenko, A.N. Composite Au nanostructures for fluorescence studies in visible light. *Nano Lett.* **2010**, *10*, 874–879.
83. Barnes, W.L. Fluorescence near interfaces: the role of photonic mode density. *J. Mod. Opt.* **1998**, *45*, 661–699.
84. Liebermann, T.; Knoll, W. Surface-plasmon field-enhanced fluorescence spectroscopy. *Colloids Surf. A* **2000**, *171*, 115–130.
85. Lakowicz, J.R.; Geddes, C.D.; Gryczynski, I.; Malicka, J.; Gryczynski, Z.; Aslan, K.; Lukomska, J.; Matveeva, E.; Zhang, J.A.; Badugu, R.; *et al.* Advances in surface-enhanced fluorescence. *J. Fluoresc.* **2004**, *14*, 425–441.

86. Fort, E.; Gresillon, S. Surface enhanced fluorescence. *J. Phys. D* **2008**, *41*, doi:10.1088/0022-3727/41/1/013001.
87. Purcell, E.M. Spontaneous emission probabilities at radio frequencies. *Phys. Rev.* **1946**, *69*, 681–681.
88. Pu, Y.; Grange, R.; Hsieh, C.L.; Psaltis, D. Nonlinear optical properties of core-shell nanocavities for enhanced second-harmonic generation. *Phys. Rev. Lett.* **2010**, doi: 10.1103/PhysRevLett.104.207402.
89. Sun, G.; Khurgin, J.B.; Soref, R.A. Practical enhancement of photoluminescence by metal nanoparticles. *Appl. Phys. Lett.* **2009**, doi:10.1063/1.3097025.
90. Xie, X.S.; Dunn, R.C. Probing single molecule dynamics. *Science* **1994**, *265*, 361–364.
91. Huang, L.; Maerkl, S.J.; Martin, O.J.F. Integration of plasmonic trapping in a microfluidic environment. *Opt. Express* **2009**, *17*, 6018–6024.
92. Gerard, J.M.; Sermage, B.; Gayral, B.; Legrand, B.; Costard, E.; Thierry-Mieg, V. Enhanced spontaneous emission by quantum boxes in a monolithic optical microcavity. *Phys. Rev. Lett.* **1998**, *81*, 1110–1113.
93. Badolato, A.; Hennessy, K.; Atature, M.; Dreiser, J.; Hu, E.; Petroff, P.M.; Imamoglu, A. Deterministic coupling of single quantum dots to single nanocavity modes. *Science* **2005**, *308*, 1158–1161.
94. Kaiser, R.; Levy, Y.; Vansteenkiste, N.; Aspect, A.; Seifert, W.; Leipold, D.; Mlynek, J. Resonant enhancement of evanescent waves with a thin dielectric waveguide. *Opt. Commun.* **1994**, *104*, 234–240.
95. Ke, P.C.; Szajman, J.; Gan, X.A.S.; Gu, M. Optimization of the enhanced evanescent wave for near-field microscopy. In *Three-Dimensional Microscopy: Image Acquisition and Processing IV*; Cogswell, C.J., Conchello, J.A., Wilson, T., Katzir, A., Eds.; SPIE-International Society for Optical Engine: Bellingham WA, USA, 1997; Volume 2984, pp. 42–49.
96. Tsang, M.; Psaltis, D. Reflectionless evanescent-wave amplification by two dielectric planar waveguides. *Opt. Lett.* **2006**, *31*, 2741–2743.
97. Kim, K.; Cho, E.J.; Huh, Y.M.; Kim, D. Thin-film-based sensitivity enhancement for total internal reflection fluorescence live-cell imaging. *Opt. Lett.* **2007**, *32*, 3062–3064.
98. Soboleva, I.V.; Descrovi, E.; Summonte, C.; Fedyanin, A.A.; Giorgis, F. Fluorescence emission enhanced by surface electromagnetic waves on one-dimensional photonic crystals. *Appl. Phys. Lett.* **2009**, *94*, doi:10.1063/1.3148671.
99. Hassanzadeh, A.; Nitsche, M.; Mittler, S.; Armstrong, S.; Dixon, J.; Langbein, U. Waveguide evanescent field fluorescence microscopy: Thin film fluorescence intensities and its application in cell biology. *Appl. Phys. Lett.* **2008**, *92*, doi:10.1063/1.2937840.
100. Budach, W.; Abel, A.P.; Bruno, A.E.; Neuschafer, D. Planar waveguides as high performance sensing platforms for fluorescence-based multiplexed oligonucleotide hybridization assays. *Anal. Chem.* **1999**, *71*, 3347–3355.
101. Lee, K.G.; Chen, X.W.; Eghlidi, H.; Kukura, P.; Lettow, R.; Renn, A.; Sandoghdar, V.; Gotzinger, S. A planar dielectric antenna for directional single-photon emission and near-unity collection efficiency. *Nat. Photonics* **2011**, *5*, 166–169.

102. Toninelli, C.; Delley, Y.; Stoferle, T.; Renn, A.; Gotzinger, S.; Sandoghdar, V. A scanning microcavity for in situ control of single-molecule emission. *Appl. Phys. Lett.* **2010**, *97*, doi:10.1063/1.3456559.
103. Begon, C.; Rigneault, H.; Jonsson, P.; Rarity, J.G. Spontaneous emission control with planar dielectric structures: An asset for ultrasensitive fluorescence analysis. *Single Mol.* **2000**, *1*, 207–214.
104. Neuschäfer, D.; Budach, W.; Wanke, C.; Chibout, S.D. Evanescent resonator chips: A universal platform with superior sensitivity for fluorescence-based microarrays. *Biosens. Bioelectron.* **2003**, *18*, 489–497.
105. Ganesh, N.; Zhang, W.; Mathias, P.C.; Chow, E.; Soares, J.; Malyarchuk, V.; Smith, A.D.; Cunningham, B.T. Enhanced fluorescence emission from quantum dots on a photonic crystal surface. *Nat. Nanotechnol.* **2007**, *2*, 515–520.
106. Zhang, W.; Cunningham, B.T. Fluorescence enhancement by a photonic crystal with a nanorod-structured high index layer. *Appl. Phys. Lett.* **2008**, *93*, doi:10.1063/1.2994696.
107. Kaji, T.; Yamada, T.; Ueda, R.; Xu, X.S.; Otomo, A. Fabrication of two-dimensional Ta₂O₅ photonic crystal slabs with ultra-low background emission toward highly sensitive fluorescence spectroscopy. *Opt. Express* **2011**, *19*, 1422–1428.
108. Liu, Y.M.; Wang, S.; Park, Y.S.; Yin, X.B.; Zhang, X. Fluorescence enhancement by a two-dimensional dielectric annular Bragg resonant cavity. *Opt. Express* **2010**, *18*, 25029–25034.
109. Norris, D.J.; KuwataGonokami, M.; Moerner, W.E. Excitation of a single molecule on the surface of a spherical microcavity. *Appl. Phys. Lett.* **1997**, *71*, 297–299.
110. Gerard, D.; Wenger, J.; Devilez, A.; Gachet, D.; Stout, B.; Bonod, N.; Popov, E.; Rigneault, H. Strong electromagnetic confinement near dielectric microspheres to enhance single-molecule fluorescence. *Opt. Express* **2008**, *16*, 15297–15303.
111. Schwartz, J.J.; Stavrakis, S.; Quake, S.R. Colloidal lenses allow high-temperature single-molecule imaging and improve fluorophore photostability. *Nat. Nanotechnol.* **2010**, *5*, 127–132.
112. Rasnik, I.; McKinney, S.A.; Ha, T. Nonblinking and longlasting single-molecule fluorescence imaging. *Nat. Methods* **2006**, *3*, 891–893.
113. Campos, L.A.; Liu, J.W.; Wang, X.A.; Ramanathan, R.; English, D.S.; Munoz, V. A photoprotection strategy for microsecond-resolution single-molecule fluorescence spectroscopy. *Nat. Methods* **2011**, *8*, 143–146.
114. Lemke, E.A.; Gambin, Y.; Vandelinder, V.; Brustad, E.M.; Liu, H.W.; Schultz, P.G.; Groisman, A.; Deniz, A.A. Microfluidic device for single-molecule experiments with enhanced photostability. *J. Am. Chem. Soc.* **2009**, *131*, 13610–13612.
115. Gambin, Y.; VanDelinder, V.; Ferreón, A.C.M.; Lemke, E.A.; Groisman, A.; Deniz, A.A. Visualizing a one-way protein encounter complex by ultrafast single-molecule mixing. *Nat. Methods* **2011**, *8*, 239–241.
116. Osborne, M.A.; Balasubramanian, S.; Furey, W.S.; Klenerman, D. Optically biased diffusion of single molecules studied by confocal fluorescence microscopy. *J. Phys. Chem. B* **1998**, *102*, 3160–3167.
117. Reisner, W.; Larsen, N.B.; Silahatoglu, A.; Kristensen, A.; Tommerup, N.; Tegenfeldt, J.O.; Flyvbjerg, H. Single-molecule denaturation mapping of DNA in nanofluidic channels. *Proc. Natl. Acad. Sci. USA* **2010**, *107*, 13294–13299.

118. Eijkel, J.C.T.; van den Berg, A. Nanofluidics: What is it and what can we expect from it? *Microfluid. Nanofluid.* **2005**, *1*, 249–267.
119. Wang, Y.C.; Stevens, A.L.; Han, J.Y. Million-fold preconcentration of proteins and peptides by nanofluidic filter. *Anal. Chem.* **2005**, *77*, 4293–4299.
120. Schoch, R.B.; Han, J.Y.; Renaud, P. Transport phenomena in nanofluidics. *Rev. Mod. Phys.* **2008**, *80*, 839–883.
121. Song, H.; Chen, D.L.; Ismagilov, R.F. Reactions in droplets in microfluidic channels. *Angew. Chem. Int. Ed.* **2006**, *45*, 7336–7356.
122. Rhoades, E.; Gussakovsky, E.; Haran, G. Watching proteins fold one molecule at a time. *Proc. Natl. Acad. Sci. USA* **2003**, *100*, 3197–3202.
123. Okumus, B.; Wilson, T.J.; Lilley, D.M.J.; Ha, T. Vesicle encapsulation studies reveal that single molecule ribozyme heterogeneities are intrinsic. *Biophys. J.* **2004**, *87*, 2798–2806.
124. Gunnarsson, A.; Jonsson, P.; Marie, R.; Tegenfeldt, J.O.; Hook, F. Single-molecule detection and mismatch discrimination of unlabeled DNA targets. *Nano Lett.* **2008**, *8*, 183–188.
125. Visnapuu, M.L.; Duzdevich, D.; Greene, E.C. The importance of surfaces in single-molecule bioscience. *Mol. Biosyst.* **2008**, *4*, 394–403.
126. Koopmans, W.J.A.; Schmidt, T.; van Noort, J. Nucleosome immobilization microscopy. *Chemphyschem* **2008**, *9*, 2002–2009.
127. Rasnik, I.; McKinney, S.A.; Ha, T. Surfaces and orientations: Much to FRET about? *Acc. Chem. Res.* **2005**, *38*, 542–548.
128. Horgan, A.M.; Moore, J.D.; Noble, J.E.; Worsley, G.J. Polymer- and colloid-mediated bioassays, sensors and diagnostics. *Trends Biotechnol.* **2010**, *28*, 485–494.
129. Dickson, R.M.; Cubitt, A.B.; Tsien, R.Y.; Moerner, W.E. On/off blinking and switching behaviour of single molecules of green fluorescent protein. *Nature* **1997**, *388*, 355–358.
130. Chrambac, A.; Rodbard, D. Polyacrylamide gel electrophoresis. *Science* **1971**, *172*, 440–451.
131. Ostuni, E.; Chapman, R.G.; Holmlin, R.E.; Takayama, S.; Whitesides, G.M. A survey of structure-property relationships of surfaces that resist the adsorption of protein. *Langmuir* **2001**, *17*, 5605–5620.
132. van Poll, M.L.; Khodabakhsh, S.; Brewer, P.J.; Shard, A.G.; Ramstedt, M.; Huck, W.T.S. Surface modification of PDMS via self-organization of vinyl-terminated small molecules. *Soft Matter* **2009**, *5*, 2286–2293.
133. Zhou, J.W.; Voelcker, N.H.; Ellis, A.V. Simple surface modification of poly(dimethylsiloxane) for DNA hybridization. *Biomicrofluidics* **2010**, *4*, doi:10.1063/1.3523055.
134. Kim, H.D.; Nienhaus, G.U.; Ha, T.; Orr, J.W.; Williamson, J.R.; Chu, S. Mg²⁺-dependent conformational change of RNA studied by fluorescence correlation and FRET on immobilized single molecules. *Proc. Natl. Acad. Sci. USA* **2002**, *99*, 4284–4289.
135. Tan, E.; Wilson, T.J.; Nahas, M.K.; Clegg, R.M.; Lilley, D.M.J.; Ha, T. A four-way junction accelerates hairpin ribozyme folding via a discrete intermediate. *Proc. Natl. Acad. Sci. USA* **2003**, *100*, 9308–9313.
136. Bentley, D.R.; Balasubramanian, S.; Swerdlow, H.P.; Smith, G.P.; Milton, J.; Brown, C.G.; Hall, K.P.; Evers, D.J.; Barnes, C.L.; Bignell, H.R.; *et al.* Accurate whole human genome sequencing using reversible terminator chemistry. *Nature* **2008**, *456*, 53–59.

137. Krieg, A.; Ruckstuhl, T.; Seeger, S. Towards single-molecule DNA sequencing: Assays with low nonspecific adsorption. *Anal. Biochem.* **2006**, *349*, 181–185.
138. Kartalov, E.P.; Unger, M.A.; Quake, S.R. Polyelectrolyte surface interface for single-molecule fluorescence studies of DNA polymerase. *Biotechniques* **2003**, *34*, 505–510.
139. Xiao, M.; Wan, E.; Chu, C.; Hsueh, W.C.; Cao, Y.; Kwok, P.Y. Direct determination of haplotypes from single DNA molecules. *Nat. Methods* **2009**, *6*, 199–201.
140. Chan, T.F.; Ha, C.; Phong, A.; Cai, D.M.; Wan, E.; Leung, L.; Kwok, P.Y.; Xiao, M. A simple DNA stretching method for fluorescence imaging of single DNA molecules. *Nucleic Acids Res.* **2006**, *34*, doi:10.1093/nar/gkl593.
141. Gomez-Sjoberg, R.; Leyrat, A.A.; Pirone, D.M.; Chen, C.S.; Quake, S.R. Versatile, fully automated, microfluidic cell culture system. *Anal. Chem.* **2007**, *79*, 8557–8563.
142. Liu, V.A.; Jastromb, W.E.; Bhatia, S.N. Engineering protein and cell adhesivity using PEO-terminated triblock polymers. *J. Biomed. Mater. Res.* **2002**, *60*, 126–134.
143. Sofia, S.J.; Premnath, V.; Merrill, E.W. Poly(ethylene oxide) grafted to silicon surfaces: Grafting density and protein adsorption. *Macromolecules* **1998**, *31*, 5059–5070.
144. Groll, J.; Amirgoulova, E.V.; Ameringer, T.; Heyes, C.D.; Rocker, C.; Nienhaus, G.U.; Moller, M. Biofunctionalized, ultrathin coatings of cross-linked star-shaped poly(ethylene oxide) allow reversible folding of immobilized proteins. *J. Am. Chem. Soc.* **2004**, *126*, 4234–4239.
145. Lee, J.N.; Park, C.; Whitesides, G.M. Solvent compatibility of poly(dimethylsiloxane)-based microfluidic devices. *Anal. Chem.* **2003**, *75*, 6544–6554.
146. Glasmaster, K.; Larsson, C.; Hook, F.; Kasemo, B. Protein adsorption on supported phospholipid bilayers. *J. Colloid Interface Sci.* **2002**, *246*, 40–47.
147. Keller, C.A.; Glasmaster, K.; Zhdanov, V.P.; Kasemo, B. Formation of supported membranes from vesicles. *Phys. Rev. Lett.* **2000**, *84*, 5443–5446.
148. Yoshina-Ishii, C.; Boxer, S.G. Arrays of mobile tethered vesicles on supported lipid bilayers. *J. Am. Chem. Soc.* **2003**, *125*, 3696–3697.
149. Graneli, A.; Yeykal, C.C.; Prasad, T.K.; Greene, E.C. Organized arrays of individual DIVA molecules tethered to supported lipid bilayers. *Langmuir* **2006**, *22*, 292–299.
150. Graneli, A.; Yeykal, C.C.; Robertson, R.B.; Greene, E.C. Long-distance lateral diffusion of human Rad51 on double-stranded DNA. *Proc. Natl. Acad. Sci. USA* **2006**, *103*, 1221–1226.
151. Greene, E.C.; Wind, S.; Fazio, T.; Gorman, J.; Visnapuu, M.L. DNA curtains for high-throughput single molecule optical imaging *Methods Enzymol.* **2010**, *472*, 293–315.
152. Harris, J.M. *Poly(ethylene glycol) Chemistry- Biotechnical and Biomedical Applications*; Harris, J.M., Ed; Plenum: New York, NY, USA, 1992.
153. Elbert, D.L.; Hubbell, J.A. Self-assembly and steric stabilization at heterogeneous, biological surfaces using adsorbing block copolymers. *Chem. Biol.* **1998**, *5*, 177–183.
154. Kim, D.; Park, S.; Lee, J.H.; Jeong, Y.Y.; Jon, S. Antibiofouling polymer-coated gold nanoparticles as a contrast agent for in vivo x-ray computed tomography imaging. *J. Am. Chem. Soc.* **2007**, *129*, 7661–7665.
155. Huang, N.P.; Voros, J.; De Paul, S.M.; Textor, M.; Spencer, N.D. Biotin-derivatized poly(L-lysine)-g-poly(ethylene glycol): A novel polymeric interface for bioaffinity sensing. *Langmuir* **2002**, *18*, 220–230.

156. Papahadjopoulos, D.; Allen, T.M.; Gabizon, A.; Mayhew, E.; Matthay, K.; Huang, S.K.; Lee, K.D.; Woodle, M.C.; Lasic, D.D.; Redemann, C.; *et al.* Sterically stabilized liposomes-improvements in pharmacokinetics and antitumour therapeutic efficacy. *Proc. Natl. Acad. Sci. USA* **1991**, *88*, 11460–11464.
157. Tanner, N.A.; van Oijen, A.M. Visualizing DNA replication at the single-molecule level. *Methods Enzymol.* **2010**, *475*, 259–278.
158. Lee, S.; Voros, J. An aqueous-based surface modification of poly(dimethylsiloxane) with poly(ethylene glycol) to prevent biofouling. *Langmuir* **2005**, *21*, 11957–11962.
159. Kenausis, G.L.; Voros, J.; Elbert, D.L.; Huang, N.P.; Hofer, R.; Ruiz-Taylor, L.; Textor, M.; Hubbell, J.A.; Spencer, N.D. Poly(L-lysine)-*g*-poly(ethylene glycol) layers on metal oxide surfaces: Attachment mechanism and effects of polymer architecture on resistance to protein adsorption. *J. Phys. Chem. B* **2000**, *104*, 3298–3309.
160. Scott, E.A.; Nichols, M.D.; Cordova, L.H.; George, B.J.; Jun, Y.S.; Elbert, D.L. Protein adsorption and cell adhesion on nanoscale bioactive coatings formed from poly(ethylene glycol) and albumin microgels. *Biomaterials* **2008**, *29*, 4481–4493.
161. Yu, L.; Li, C.M.; Liu, Y.S.; Gao, J.; Wang, W.; Gan, Y. Flow-through functionalized PDMS microfluidic channels with dextran derivative for ELISAs. *Lab Chip* **2009**, *9*, 1243–1247.
162. Massia, S.P.; Stark, J.; Letbetter, D.S. Surface-immobilized dextran limits cell adhesion and spreading. *Biomaterials* **2000**, *21*, 2253–2261.
163. Zhang, Z.W.; Feng, X.J.; Xu, F.; Liu, X.; Liu, B.F. "Click" chemistry-based surface modification of poly(dimethylsiloxane) for protein separation in a microfluidic chip. *Electrophoresis* **2010**, *31*, 3129–3136.
164. Wang, A.J.; Xu, J.J.; Chen, H.Y. In-situ grafting hydrophilic polymer on chitosan modified poly(dimethylsiloxane) microchip for separation of biomolecules. *J. Chromatogr.* **2007**, *1147*, 120–126.
165. Zhang, Z.W.; Feng, X.J.; Luo, Q.M.; Liu, B.F. Environmentally friendly surface modification of PDMS using PEG polymer brush. *Electrophoresis* **2009**, *30*, 3174–3180.
166. Heyes, C.D.; Groll, J.; Moller, M.; Nienhaus, G.U. Synthesis, patterning and applications of star-shaped poly(ethylene glycol) biofunctionalized surfaces. *Mol. Biosyst.* **2007**, *3*, 419–430.
167. Xiao, Y.; Yu, X.D.; Xu, J.J.; Chen, H.Y. Bulk modification of PDMS microchips by an amphiphilic copolymer. *Electrophoresis* **2007**, *28*, 3302–3307.
168. Zhou, J.H.; Yan, H.; Ren, K.N.; Dai, W.; Wu, H.K. Convenient method for modifying poly(dimethylsiloxane) with poly(ethylene glycol) in microfluidics. *Anal. Chem.* **2009**, *81*, 6627–6632.
169. Hu, S.W.; Ren, X.Q.; Bachman, M.; Sims, C.E.; Li, G.P.; Allbritton, N. Surface modification of poly(dimethylsiloxane) microfluidic devices by ultraviolet polymer grafting. *Anal. Chem.* **2002**, *74*, 4117–4123.
170. Sebra, R.P.; Masters, K.S.; Cheung, C.Y.; Bowman, C.N.; Anseth, K.S. Detection of antigens in biologically complex fluids with photografted whole antibodies. *Anal. Chem.* **2006**, *78*, 3144–3151.
171. Kim, P.; Jeong, H.E.; Khademhosseini, A.; Suh, K.Y. Fabrication of non-biofouling polyethylene glycol micro- and nanochannels by ultraviolet-assisted irreversible sealing. *Lab Chip* **2006**, *6*, 1432–1437.

172. Han, J.-H.; Yoon, J.-Y. Reusable, polyethylene glycol-structured microfluidic channels for particle immunoassays. *J. Biol. Eng.* **2009**, *3*, 1–6.
173. Xu, Y.H.; Yang, X.R.; Wang, E.K. Review: Aptamers in microfluidic chips. *Anal. Chim. Acta* **2010**, *683*, 12–20.

© 2011 by the authors; licensee MDPI, Basel, Switzerland. This article is an open access article distributed under the terms and conditions of the Creative Commons Attribution license (<http://creativecommons.org/licenses/by/3.0/>).